DOI: 10.17344/acsi.2017.3953 *Acta Chim. Slov.* **2018,** *65,* 312–318
creative commons

Scientific paper

Effect of Copper Alloying on Electro-Catalytic Activity of Nickel for Ethanol Oxidation in Alkaline Media

Niloufar Bahrami Panah,[1,*] Iman Danaee,[2] Mahmood Payehghadr[1] and Afrooz Madahi[1]

[1]*Department of Chemistry, Payame Noor University, P.O.BOX 19395-3697, Tehran, Iran*

[2]*Abadan Faculty of Petroleum Engineering, Petroleum University of Technology, Abadan, Iran*

** Corresponding author: E-mail: bahramipanah@pnu.ac.ir*
Tel.: +982634209515 Fax: +982634209525

Received: 03-11-2017

Abstract

In this research, the electro-catalytic activity of nickel-copper (Ni-Cu) alloy towards oxidation of ethanol and its possible redox process were investigated in alkaline solution. For this purpose, cyclic voltammetry, chronoamperometry and electrochemical impedance spectroscopy techniques were employed. According to the cyclic voltammetry studies, Ni-Cu alloy compared to pure nickel can demonstrate a significantly higher response for ethanol oxidation. So, the enhancement of the anodic peak current corresponding to the oxidation of nickel hydroxide was accompanied with attenuated cathodic current in the presence of ethanol. The anodic peak currents have a linearly dependence on the square root of scan rate which is the characteristic of diffusion-controlled processes. Based on the chronoamperometry measurements, the reaction exhibited a Cottrellian behavior and the diffusion coefficient of ethanol was found to be 1.26×10^{-5} cm^2 s^{-1}. The impedance spectroscopy declared electro-catalytic behavior of Ni-Cu electrode for oxidation of ethanol and showed that the charge transfer resistance decreases by increasing the ethanol concentration.

Keywords: Electro-catalytic activity; nickel-copper alloy; ethanol; impedance

1. Introduction

Recently, direct ethanol fuel cells (DEFCs) have attracted much interest for different applications.[1,2] The reason is that they can provide convenient operation, storage and distribution. However, DEFCs require further development compared to hydrogen based fuel cells.[3] One of the unresolved problems of DEFCs is slow anodic rate of ethanol oxidation.[4] In this respect, considerable researches have been devoted to study ethanol electro-oxidation at high pH values. Utilizing alkaline solution has many advantages in fuel cells. For example, it can enhance fuel cell efficiency, reduce corrosion, enable the application of many electrode materials, promote efficiency of the processes occured at both anode and cathode, eliminate sensitivity to the surface structure and decrease poisoning effects.[5–8]

In electrochemical oxidation of ethanol, selection of an appropriate material for the anode is very crucial for obtaining an electro-catalyst of high efficiency. Some studies have reported a significant increase in fuel utilization and power density through optimizing different factors related to fuel cells.[9,10] For the electrode, different materials have been employed to catalyze the electrochemical oxidation of ethanol.[11,12] One of the well-established electrode materials is nickel which poses proper surface oxidation properties. Nickel and its complexes have been commonly applied in electro-catalysis to proceed both anodic and cathodic reactions in water electrolysis and organic synthesis.[13–17] One of the remarkable applications of nickel is catalyzing the ethanol oxidation. Several studies regarding to electro-oxidation of alcohols on nickel electrode have been reported.[18–20]

For obtaining a synergistic electro-catalytic system, the nickel alloys specifically nickel-copper can be used.[21–23] In addition, alloy electrodes compared to other electro-catalysts can offer further advantages such as long-term stability and ease of preparation. The crystal structures of pure Ni and Cu metals are similar and they possess face-centered cubic structures with similar lattice parameters. Therefore, it is possible to make a wide range of Ni-Cu alloy ratios.[24–27]

The aim of present work is to study the electrochemical oxidation of ethanol on Ni-Cu alloy (70/30) electrode in alkaline solution and compare its catalytic activity with pure Ni electrode via electrochemical techniques of cyclic voltammetry, chronoamperometry and impedance spectroscopy.

2. Experimental

All chemicals used in this work [Sodium hydroxide and ethanol in analytical grade] were of Merck origin (Germany) and used without further purification. Double distilled water was employed to prepare the solutions. Nickel and nickel-copper alloy were prepared from Rooyingran Sanaat Company. The electrochemical measurements were carried out in a one-compartment three-electrode cell powered by a Metrohm-Autolab potentiostat/galvanostat (model 12/30/302, The Netherlands). The disk of Ni-Cu alloy (70/30) of 1 cm^2 area was employed as working electrode. Before each measurement, the electrode was polished with emery paper of 1000 grit and rinsed in double distilled water and acetone. Counter and reference electrodes were platinum and KCl-saturated Ag/AgCl electrode (Metrohm, The Netherlands), respectively. All the electrochemical studies were done at 22 ± 1 °C.

The electrochemical impedance experiments were carried out in a frequency range of 100 kHz to 10 mHz and modulation amplitude of 10 mV with respect to open circuit potential. The experimental impedance spectroscopy data were fitted to the proposed equivalent circuit using a home written least square software. This software was programmed according to the method of Marquardt for optimization of functions and Macdonald weighting for the real and imaginary parts of the experimental impedance data.[28,29]

3. Results and Discussion

Figure 1 displays consecutive cyclic voltammograms of the Ni-Cu electrode in 1 M NaOH solution recorded after 50 cycles at scan rate of 100 mV s^{-1}. Upon the first scan, a pair of redox peak is observed at 463 and 295 mV which is attributed to the Ni^{2+}/Ni^{3+} redox couple. In the subsequent cycles, the anodic and cathodic peaks shift to the negative direction and stabilize at 378 and 310 mV, respectively. This behavior is consistent with the data reported in previous electrochemical studies related to formation of the nickel oxide film on the surface and inter-conversion of α-$Ni(OH)_2$ and ß-phases, conversion of $Ni(OH)_2$ to NiOOH and enrichment of Ni^{3+} species around the surface of the electrode.[30,31] During the next cycles, a negative shift of the anodic peak and its stabilization are evident, which refer to higher potential energies required for NiOOH nucleation. In the first cycle, the baseline current is higher which corresponds to the oxidation of Ni to Ni^{2+}. An increase in peak currents with the number of cycles demonstrates a continuous enrichment of electrode's surface by accessible Ni^{2+} and Ni^{3+}electro-active species. Figure 2 shows the cyclic voltammograms of the Ni, Cu and Ni-Cu electrode in 1 M NaOH solution recorded at scan rate of 10 mV s^{-1}. As can be seen, the oxidation behavior of Ni and Ni-Cu electrode is the same and the Ni^{2+}/Ni^{3+} redox couple is observed. No considerable anodic peak for Cu^{3+} is shown in cyclic voltammogram of Cu electrode, but the cathodic peak is clear in inset of Figure 2.

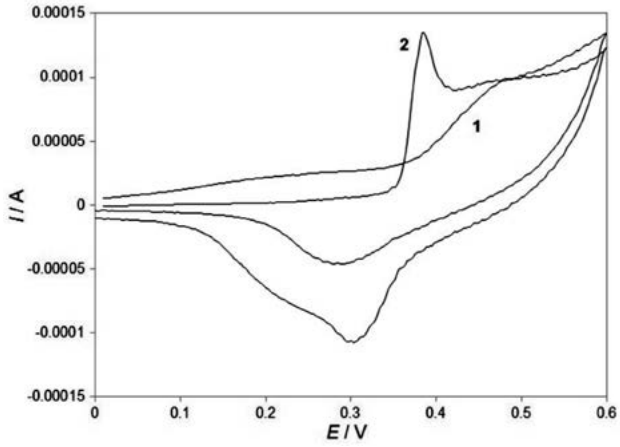

Figure 1. Consecutive cyclic voltammogram of Ni-Cu electrode oxidation in 1 M NaOH (1) first and (2) fiftieth cycle at a scan rate of 100 mV s^{-1}.

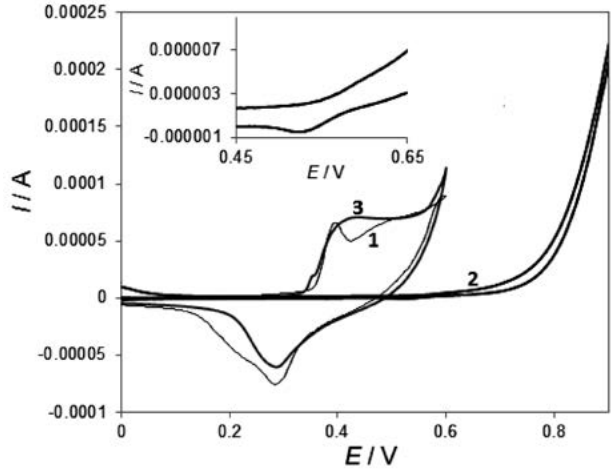

Figure 2. Cyclic voltammogram of (1) Ni, (2) Cu and (3) Ni-Cu electrode oxidation in 1 M NaOH at a scan rate of 10 mV s^{-1}. Unset: Cyclic voltammogram of Cu electrode in the potential range of 0.45 and 0.65 V.

Figure 3a illustrates the typical cyclic voltammograms of a Ni-Cu electrode at various scan rates (2–2500 mV s^{-1}) in 1 M NaOH solution. Figure 3b shows that the anodic peak currents increase proportional to the lower

scan rate values (2–200 mV s^{-1}). This behavior is expected for the electrochemical activity of redox couples that their voltammetric responses are sensitive to the low concentration of surface-confined electro-active species.[32] In this process, only the nickel oxide layer produced on electrode surface participates in the redox reaction.[33] Surface coverage of the redox species, Γ*, can be calculated according to the slope of the lines shown in Figure 3b:[33]

$$I_p = \left(\frac{n^2F^2}{4RT}\right) vA\Gamma^* \quad (1)$$

where I_p, n, and *v* is peak current, electron transfer number and potential scan rate, respectively. The Γ* value is calculated to be about 8.15 × 10^{-8} mol cm^{-2} which is related to the presence of ca. 80 monolayers of surface species on Ni-Cu electrode. Figure 3c presents the proportionality of anodic peak current to square root values of higher scan rates (350–2500 mV s^{-1}). It shows that the oxidation reaction is a diffusion-controlled process at higher scan rate[33] and the reaction is limited by diffusion of hydroxide ion from bulk of solution to the electrode surface according to following equation:

$$Ni(OH)_2 + OH^- \rightleftharpoons NiOOH + H_2O + e \quad (2)$$

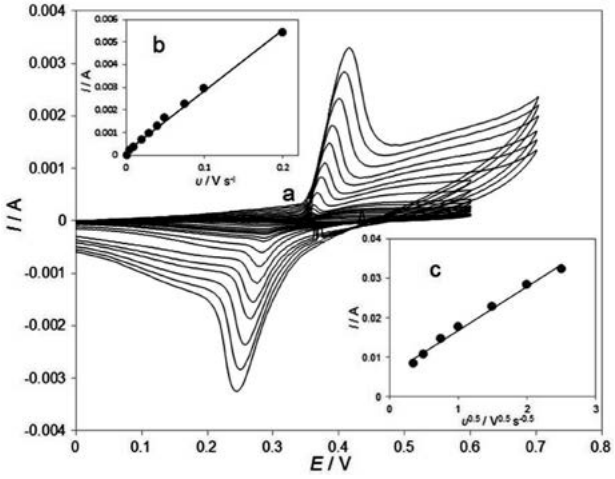

Figure 3. (a) Typical cyclic voltammograms of Ni-Cu electrode in 1 M NaOH at different scan rates of 2–2500 mV s^{-1}, (b) The dependency of anodic peak currents to the scan rate at lower values (2–200 mV s^{-1}), (c) The proportionality of anodic peak currents to the square roots of scan rate at higher values (350–2500 mV s^{-1}).

Figure 4 depicts cyclic voltammograms of pure Ni, pure Cu and Ni-Cu electrodes in 1 M NaOH solution containing 0.5 M ethanol at scan rate of 10 mV s^{-1}. As seen, Ni-Cu electrode provides a higher current density for ethanol electro-oxidation in alkaline solution. The reason can be related to higher atomic radius of Cu compared to Ni which can enhance ethanol adsorption on the electrode surface. Furthermore, electro-catalytic activity of Cu electrode is high for ethanol oxidation, but it is at higher anodic over-potentials. As it can be seen, the measured anodic potentials of Ni-Cu and Ni electrodes are the same, but the anodic peak current of Ni-Cu is higher than that in Ni electrode. Consequently, the high electro-catalytic activity of Cu electrode is responsible for electro-catalytic activity of Ni-Cu electrode.

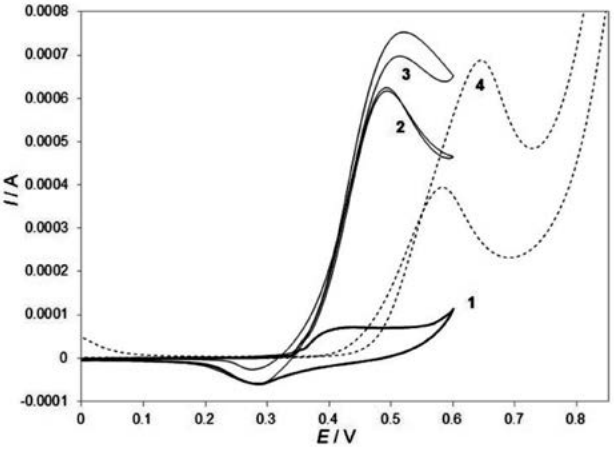

Figure 4. Cyclic voltammograms in the (1) absence and (2) presence of 0.5 M ethanol on Ni, (3) Ni-Cu (4) Cu electrode in 1 M NaOH solution. Scan rate: 10 mV s^{-1}.

Figure 5a exhibits the cyclic voltammograms of Ni-Cu electrode in a solution of 1 M NaOH and different concentrations of ethanol at scan rate of 10 mV s^{-1}. It is declared that the oxidation of ethanol on Ni-Cu electrode has a typical electro-catalytic response. The anodic current increases around the potential of 350 mV. The oxidation of ethanol and Ni^{2+} oxidation to Ni^{3+} starts simultaneously. The anodic to cathodic charge ratio in the presence of 0.5 M ethanol is obtained to be 92/8 while it is 55/45 in the absence of ethanol. The charge values are calculated through integrating the background corrected anodic and cathodic peaks.

In the positive sweep, the measured anodic current is proportional to the bulk concentration of ethanol. An increase in ethanol concentration up to 0.6 M caused a linear increase in the anodic current (Figure 5b). Based on these evidences, catalytic electro-oxidation of ethanol on Ni-Cu electrode is confirmed. Zhang et al. investigated the ethanol oxidation on Ni-B amorphous alloy nanoparticles modified nanoporous Cu in alkaline medium.[34] They reported that ethanol oxidation at the Ni-B modified porous Cu electrode had a negative shift of 52 mV in the onset oxidation potential and the oxidation peak current increased in comparison with the bulk Ni. Kakaei and Marzang studied the electro-catalytic activity of nitrogen doped reduced graphene oxide with Ni-Co nanoparticles for ethanol oxidation in alkaline media.[35] The fabricated alloy electro-catlyst exhibited a remark-

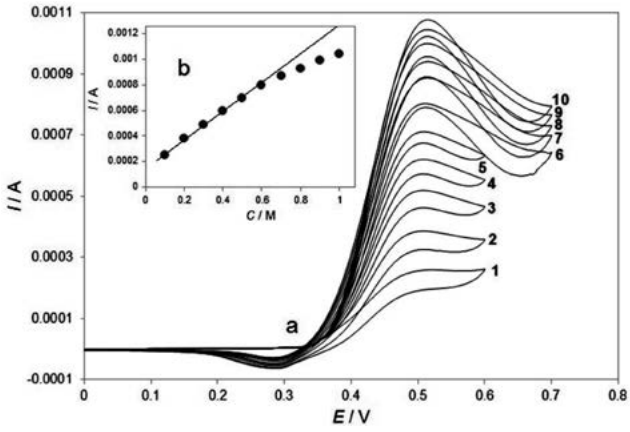

Figure 5. (a) Cyclic voltammograms of the Ni-Cu electrode in 1 M NaOH solution in the presence of (1) 0.1, (2) 0.2, (3) 0.3, (4) 0.4, (5) 0.5, (6) 0.6, (7) 0.7, (8) 0.8, (9) 0.9 and (10) 1 M of ethanol. Scan rate: 10 mV s^{-1}. (b) Dependency of the anodic peak current on the concentration of ethanol.

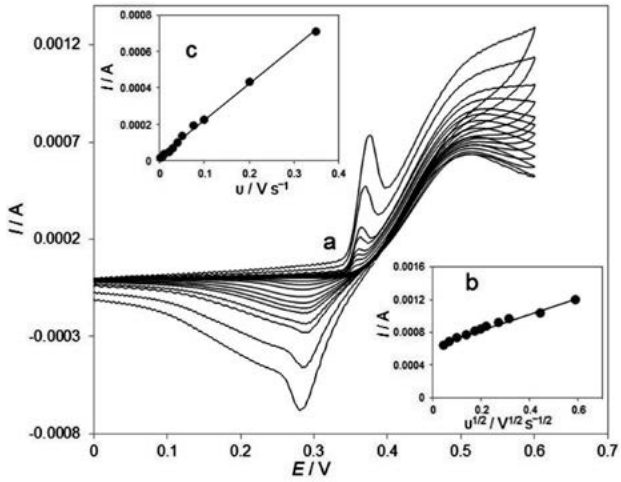

Figure 6. (a) Typical cyclic voltammograms of the Ni-Cu in 1 M NaOH in the presence of 0.5 M ethanol at various scan rates of 2, 5, 10, 20, 30, 40, 50, 75, 100, 200 and 350 mV s^{-1}. (b) Dependence of anodic peak current at 530 mV on the square root of scan rate. (c) Dependence of anodic peak current at 370 mV on the scan rate.

able electro-catalytic activity and high stability for the ethanol oxidation reaction in comparison with fabricated Ni and Co.

The decrease in cathodic current that occurs in the negative potential scan verifies the involvement of ethanol in the rate determining step. It also indicates that the process is incapable of reducing all high-valence nickel species that have formed in the anodic half cycle. Along with the oxidation of Ni^{2+}species to Ni^{3+}, the adsorbed ethanol molecules oxidize on the surface at higher over-potentials. The products or intermediates of the reaction poison the electrode surface and reduces the number of available sites for ethanol adsorption. Consequently, the anodic current approaches a maximum in the positive potential scan and then the overall rate of ethanol oxidation decreases. Electro-catalytic oxidation of ethanol also continues in the early stages of the cathodic half cycle and the current tends to a maximum since some active sites for adsorption of ethanol regenerate due to removal of the adsorbed intermediates and products.

Figure 6 shows the cyclic voltammograms of Ni-Cu electrode in the presence of 0.5 M ethanol at various potential scan rates (2–350 mV s^{-1}) and also the scan rate proportionality of the anodic peak current. The anodic peak potential appears at 0.5 V as a result of ethanol oxidation on the nickel active sites. The variation of anodic peak current vs. the square root of scan rate values shows a linear relationship which represents that the oxidation of ethanol on Ni-Cu electrode is controlled by diffusion of ethanol species from solution to the redox sites accessible on the electrode's surface (Figure 6b). Although, the cathodic peak of Ni^{3+} reduction is negligible at low scan rates, but it appears at higher scan rates. This observation implies that the electro-oxidation of nickel species is much faster than catalytic oxidation of ethanol at higher scan rates. Therefore, oxidation of ethanol on nickel surface is a slow process.

At higher scan rates, the oxidation peak of $Ni(OH)_2$ to NiOOH rises at potentials that are considerably more negative than the potential of ethanol oxidation (≈ 370 mV). This peak is insignificant at low scan rates but enhances at higher scan rate values. Figure 6c illustrates a linear dependency of the current peak on the scan rate which proposes the presence of surface-confined electro-active species. According to the high current density observed in the presence of ethanol and also the appearance of two oxidation peaks for Ni^{2+} and ethanol, it is appeared that one of the anodic current can be attributed to the oxidation of ethanol by NiOOH since the NiOOH reduction peak disappears during the negative scan. The other one can be assigned to the direct electro-oxidation of ethanol on the surface of the oxide layer.

The following redox reaction of the nickel species is expected:

$$Ni(II) \rightarrow Ni(III) + e \quad (3)$$

while ethanol oxidizes on the alloy surface through the following reaction [23,36,37]:

$$Ni^{3+} + \text{ethanol} \rightarrow Ni^{2+} + \text{intermediate} \quad (4)$$

$$Ni^{3+} + \text{intermediate} \rightarrow Ni^{2+} + \text{product} \quad (5)$$

In Eqs. (4) and (5), ethanol oxidation occurs through the reduction of NiOOH sites. The Ni^{3+} sites can be regenerated by the power source or via direct electro-oxidation on Ni^{3+} oxide surface as follows:

$$Ni^{3+} - \text{ethanol} \rightarrow Ni^{3+} - \text{intermediate} + e \quad (6)$$

$$Ni^{3+} - \text{intermediate} \rightarrow Ni^{3+} - \text{product} + e \quad (7)$$

In Eqs. (6) and (7), Ni^{3+} provides an active site for direct ethanol oxidation. Also, Eqs. (3), (6) and (7) refer to two anodic peaks of ethanol and Ni^{2+} oxidation.

Figure 7a displays the chronoamperograms recorded for Ni-Cu in 1 M NaOH solution containing (0.1–0.8 M) ethanol at the potential step of 500 mV. Figure 7b identifies a linear behavior of the net current changes (after elimination of the background current) vs. the inverse square root of time. So, a diffusion-controlled process is dominant in this electrochemical process. The diffusion coefficient of ethanol is calculated 1.26×10^{-5} cm^2 s^{-1} by substitution of the line slope of Figure 7b into Cottrell equation[33] (Eq. 8).

$$I = nFAD^{1/2}C\pi^{-1/2}t^{-1/2} \quad (8)$$

The catalytic rate constant of ethanol oxidation on Ni-Cu alloy is evaluated according to Eq. (9) which is introduced by Pariente et al.:[38]

$$\frac{I_{catal}}{I_d} = \gamma^{1/2}\left(\pi^{1/2}erf(\gamma^{1/2}) + \frac{\exp(-\gamma)}{\gamma^{1/2}}\right) \quad (9)$$

Where I_{catal} and I_d stand for Ni-Cu electrode currents in the presence and absence of ethanol, respectively. $y = kCt$ is the related error function in which k is the catalytic rate constant, C is the bulk concentration of ethanol and t is the elapsed time. When $y\rangle 1.5$, $erf\,(y^{1/2})$ equals to unity approximately and Eq. (9) simplifies to:

$$\frac{I_{catal}}{I_d} = \gamma^{1/2}\pi^{1/2} = \pi^{1/2}(kCt)^{1/2} \quad (10)$$

Based on the slope of I_{catal}/I_d vs. $t^{1/2}$ plot, the obtained mean catalytic rate constant was 865.5 cm^3 mol^{-1} s^{-1} for ethanol concentration of 0.1–0.8 M (Figure 7c).

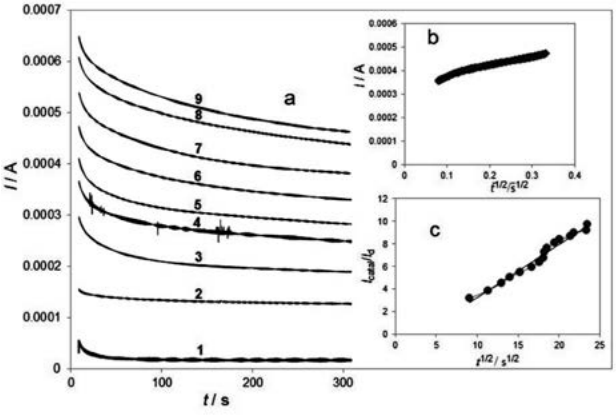

Figure 7. (a) Chronoamperograms of Ni-Cu electrode in 1 M NaOH solution with different concentration of ethanol: (1) blank, (2) 0.1, (3) 0.2, (4) 0.3, (5) 0.4, (6) 0.5, (7) 0.6, (8) 0.7 and (9) 0.8 M at potential step of 500 mV. (b) Dependency of transient current on $t^{-1/2}$. (c) Dependence of I_{catal}/I_d vs. $t^{1/2}$ derived from the data of chronoamperograms.

Figure 8 represents the Nyquist diagrams of Ni-Cu electrode recorded at the anodic peak potential as the dc-offset in 1 M NaOH solution containing different concentration of ethanol. These diagrams contain two depressed semicircles that are overlapped. The high frequency depressed semicircle corresponds to a combination of a charge transfer resistance and the double layer capacitance and the low frequency semicircle can be due to the adsorption of reaction intermediate on the surface of Ni-Cu electrode.[39,40]

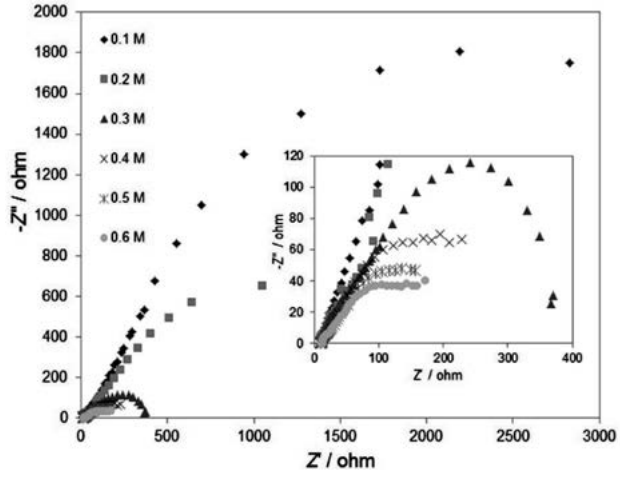

Figure 8. Nyquist diagrams of Ni-Cu electrode in 1 M NaOH solution containing different concentration of ethanol at an anodic potential of 500 mV. Inset: high frequency part of the Nyquist diagram.

Figure 9 shows the equivalent circuit in the presence of ethanol which is compatible with Nyquist diagram. The capacitor C should be replaced with a constant phase element (CPE), Q, in the equivalent circuit. The CPE behavior is due to the microscopic roughness of the electrode that causes an inhomogeneous distribution in the solution resistance and the double-layer capacitance.[41,42] In Figure 9, R_s, Q_{dl} and R_{ct} are solution resistance, a constant phase

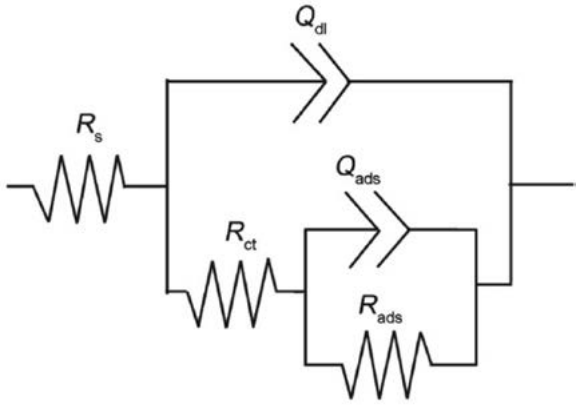

Figure 9. Equivalent circuit compatible with the experimental impedance data in Figures 8 for ethanol electro-oxidation on Ni-Cu electrode.

Table 1. Equivalent circuit parameters of electro-oxidation of ethanol on Ni-Cu electrode in 1 M NaOH solution.

Concentration / M	R_s / Ω	R_{ct} / Ω	Q_{dl} / F	n_1	R_{ads} / Ω	Q_{ads} / F	n_2
0.1	11.9	105	0.0018	0.79	4224	0.008	0.9
0.2	11.5	78	0.0024	0.79	1671	0.018	0.75
0.3	11.7	45	0.0026	0.77	361	0.018	0.68
0.4	10.3	21	0.0025	0.67	274	0.02	0.56
0.5	10.5	19	0.003	0.66	196	0.025	0.58
0.6	10.9	18	0.003	0.67	181	0.03	0.57

element related to the double layer capacitance and charge transfer resistance, respectively. Also, Q_{ads} and R_{ads} are the electrical elements corresponding to the adsorption of reaction intermediates.

The experimental data were fitted to the equivalent circuit to obtain the circuit elements. Table 1 represents the equivalent circuit parameters for the impedance spectra of ethanol electro-oxidation. The charge transfer resistance value decreases as the ethanol concentration increases. It approves the catalytic activity of Ni-Cu alloy for ethanol oxidation. n_1 and n_2 are the constant phase element exponent and show the extent of difference between capacitance and the constant phase element.

4. Conclusions

In this study, the electro-oxidation of ethanol was investigated on the nickel oxide film formed on the surface of Ni-Cu alloy electrode in an alkaline solution. The results confirmed that Ni-Cu alloy is electro-catalytically active for ethanol oxidation at a potential of ≈ 500 mV. The catalytic response obtained for electro-oxidation of ethanol on Ni-Cu electrode is greater than the one observed for pure nickel. The anodic peak currents for ethanol oxidation are linearly proportional to square root of scan rates. The chronoamperograms revealed the dominance of a diffusion-controlled process in presence of ethanol species. The diffusion coefficient of ethanol was calculated 1.26 $\times 10^{-5}$ cm^2 s^{-1}. The charge transfer resistance for various concentrations of ethanol was evaluated and highlighted an effective catalytic activity of Ni-Cu alloy for oxidation of ethanol in alkaline solutions.

5. References

1. Y. Li, Z. Wang, X. Li, T. Yin, K. Bian, F. Gao, D. Gao, *J. Power Sources* **2017**, *341*, 183–191. **DOI:**10.1016/j.jpowsour.2016.12.006
2. Q. Zhang, F. Zhang, X. Ma, Y. Zheng, S. Hou, *J. Power Sources* **2016**, *336*, 1–7. **DOI:**10.1016/j.jpowsour.2016.10.028
3. Z. Xiong, B. Yan, K. Zhang, C. Wang, S. Li, H. Xu, Y. Du, C. Zhai, *J. Taiwan Inst. Chem. E.* **2017**, 75, 12–17. **DOI:**10.1016/j.jtice.2017.03.008
4. Y. Xie, H. Zhang, G. Yao, S. A. Khan, X. Cui, M. Gao, Y. Lin, *J. Energy Chem.* **2017**, *26*, 193–199. **DOI:**10.1016/j.jechem.2016.11.014
5. J. L. Tan, A. M. De Jesus, S. L. Chua, J. Sanetuntikul, S. Shanmugam, B. J. V. Tongol, H. Kim, *Appl. Catal. A- Gen.* **2017**, *531*, 29–35. **DOI:**10.1016/j.apcata.2016.11.034
6. C. Peng, W. Yang, E. Wu, Y. Ma, Y. Zheng, Y. Nie, H. Zhang, J. Xu, *J. Alloy Compd.* **2017**, *698*, 250–258. **DOI:**10.1016/j.jallcom.2016.12.198
7. Y. H. Qin, Z. Y. Xiong, J. Ma, L. Yang, Z. Wu, W. Feng, T. L. Wang, W. G. Wang, C. W. Wang, *Int. J. Hydrogen Energ.* **2017**, *42*, 1103–1112. **DOI:**10.1016/j.ijhydene.2016.09.060
8. T. Li, G. Fu, J. Su, Y. Wang, Y. Lu, X. Zou, X. Zhu, L. Xu, D. Sun, Y. Tang, *Electrochim. Acta* **2017**, *231*, 13–19. **DOI:**10.1016/j.electacta.2017.02.044
9. X. Hu, C. Lin, L. Wei, C. Hong, Y. Zhang, N. Zhuang, *Electrochim. Acta* **2016**, *187*, 560–566. **DOI:**10.1016/j.electacta.2015.11.100
10. C. Du, X. Gao, Z. Zhuang, C. Cheng, F. Zheng, X. Li, W. Chen, *Electrochim. Acta* **2017**, *238*, 263–268. **DOI:**10.1016/j.electacta.2017.03.198
11. P. Kanninen, N. D. Luong, L. H. Sinh, J. Flórez-Montaño, H. Jiang, E. Pastor, J. Seppälä, T. Kallio, *Electrochim. Acta* **2017**, *242*, 315–326. **DOI:**10.1016/j.electacta.2017.05.019
12. K. Ding, P. Wang, J. Zhao, Y. Li, Y. Chen, Y. Zhang, B. Wei, Y. Sun, J. Pan, *Int. J. Hydrogen Energ.* **2017**, *42*, 9766–9774. **DOI:**10.1016/j.ijhydene.2017.01.210
13. I. Danaee, M. Jafarian, F. Forouzandeh, F. Gobal, *Int. J. Chem. Kinet.* **2012**, *44*, 712–721. **DOI:**10.1002/kin.20721
14. J. Guo, Y. Hou, B. Li, E. Duan, *Mater. Lett.* **2017**, *200*, 90–93. **DOI:**10.1016/j.matlet.2017.04.111
15. I. Danaee, M. Jafarian, M. Sharafi, F. Gobal, *J. Electrochem. Sci. Technol.* **2012**, 3, 50–56. **DOI:**10.5229/JECST.2012.3.1.50
16. W. Shi, Q. Wang, F. Qin, J. Yu, M. Jia, H. Gao, Y. Zhang, Y. Zhao, G. Li, *Electrochim. Acta* **2017**, *232*, 332–338. **DOI:**10.1016/j.electacta.2017.02.164
17. W. Shi, H. Gao, J. Yu, M. Jia, T. Dai, Y. Zhao, J. Xu, G. Li, *Electrochim. Acta* **2016**, *220*, 486–492. **DOI:**10.1016/j.electacta.2016.10.051
18. S. J. Zhang, Y. X. Zheng, L. S. Yuan, L. H. Zhao, *J. Power Sources* **2014**, *247*, 428–436. **DOI:**10.1016/j.jpowsour.2013.08.129
19. N. A. M. Barakat, H. M. Moustafa, M. M. Nassar, M. A. Ab-

delkareem, M.S. Mahmoud, A. A. Almajid, K. A. Khalil, *Electrochim. Acta* **2015**, *182*, 143–155. **DOI:**10.1016/j.electacta.2015.09.079
20. K. Kakaei, K. Marzang, *J. Colloid Interf. Sci.* **2016**, *462*, 148–153. **DOI:**10.1016/j.jcis.2015.09.072
21. I. Pötzelberger, A. I. Mardare, A. W. Hassel, *Appl. Surf. Sci.* **2017**, *417*, 48–53. **DOI:**10.1016/j.apsusc.2016.12.193
22. I. Danaee, M. Jafarian, F. Forouzandeh, F. Gobal, M. G. Mahjani, *Int. J. Hydrogen Energy* **2008**, *33*, 4367–4376. **DOI:**10.1016/j.ijhydene.2008.05.075
23. I. Danaee, M. Jafarian, F. Forouzandeh, F. Gobal, M. G. Mahjani, *Int. J. Hydrogen Energy* **2009**, *34*, 859–869. **DOI:**10.1016/j.ijhydene.2008.10.067
24. M. Jafarian, T. Rostami, M. G. Mahjani, F. Gobal, *J. Electroanal. Chem.* **2016**, *763*, 134–140. **DOI:**10.1016/j.jelechem.2015.12.031
25. S. J. Zhang, Y. X. Zheng, L. S. Yuan, L. H. Zhao, *J. Power Sources* **2014**, *247*, 428–436. **DOI:**10.1016/j.jpowsour.2013.08.129
26. L. Wang, X. Lu, Y. Ye, L. Sun, Y. Song, *Electrochim.Acta* **2013**, *114*, 484–493. **DOI:**10.1016/j.electacta.2013.10.125
27. X. Tarrús, M. Montiel, E. Vallés, E. Gómez, *Int. J. Hydrogen Energ.* **2014**, *39*, 6705–6713. **DOI:**10.1016/j.ijhydene.2014.02.057
28. J. R. Macdonald, *Solid State Ionics* **1984**, *13*, 147–149. **DOI:**10.1016/0167-2738(84)90049-3
29. I. Danaee, S. Noori, *Int. J. Hydrogen Energ.* **2011**, *36*, 12102–12111. **DOI:**10.1016/j.ijhydene.2011.06.106
30. F. Hahn, B. Beden, M. J. Croissant, C. Lamy, *Electrochim. Acta* **1986**, *31*, 335. **DOI:**10.1016/0013-4686(86)80087-1
31. A. A. El-Shafei, *J. Electroanal. Chem.* **1999**, *471*, 89–95. **DOI:**10.1016/S0022-0728(99)00235-1
32. R. Barnard, C. F. Randell, *J. Appl. Electrochem.* **1983**, *13*, 89–95. **DOI:**10.1007/BF00615892
33. A. J. Bard, L. R. Faulkner (Ed.): Electrochemical Methods: Fundamentals and Applications, Wiley, New York, **2001**, pp. 591.
34. S. J. Zhang, Y. X. Zheng, L. S. Yuan, L. H. Zhao, *J. Power Sources* **2014**, *247*, 428–436. **DOI:**10.1016/j.jpowsour.2013.08.129
35. K. Kakaei, K. Marzang, J. Colloid Interf. Sci. **2016**, *462,* 148–153. **DOI:**10.1016/j.jcis.2015.09.072
36. I. Danaee, M. Jafarian, F. Forouzandeh, F. Gobal, M.G. Mahjani, *Electrochim. Acta* **2008**, *53*, 6602–6609. **DOI:**10.1016/j.electacta.2008.04.042
37. I. Danaee, M. Jafarian, F. Forouzandeh, F. Gobal, M.G. Mahjani, *J. Phys. Chem. B* **2008**, *112*, 15933–15940. **DOI:**10.1021/jp8069173
38. F. Pariente, E. Lorenzo, F. Tobalina, H. D. Abruna, *Anal. Chem.* **1995**, *67*, 3936–3944. **DOI:**10.1021/ac00117a019
39. I. Danaee, M. Jafarian, F. Gobal, M. Sharafi, M. G. Mahjani, *Chem. Res. Chinese U.* **2012**, *28*, 19–25.
40. M. Jafarian, A. Mirzapoor, I. Danaee, A. A. Shahnazi Sangachin, F. Gobal, *Sci. China Chem.* **2012**, *55*, 1819–1824. **DOI:**10.1007/s11426-012-4731-6
41. H. Jafari, I. Danaee, H. Eskandari, M. Rashvand Avei, *J. Mater. Sci. Technol.* **2014**, *30*, 239–252. **DOI:**10.1016/j.jmst.2014.01.003
42. A. R. Hosein Zadeh, I. Danaee, M. H. Maddahy, *J. Mater. Sci. Technol.* **2013**, *29*, 884–892. **DOI:**10.1016/j.jmst.2013.06.006

Povzetek

V tej raziskavi smo v alkalni raztopini raziskali elektrokatalitsko aktivnost elektrode iz zlitine nikelj-baker (Ni-Cu) za oksidacijo etanola in njegovega morebitnega procesa redukcije. V ta namen smo uporabili ciklično voltametrijo, kronoamperometrijo in tehniko elektrokemijske impedančne spektroskopije. Rezultati študije ciklične voltametrije kažejo na povečano oksidacijo etanola v primeru uporabe zlitine Ni-Cu v primerjavi z uporabo samo nikljeve elektrode. Povečanje anodnega vrha, ki ustreza oksidaciji nikljevega hidroksida, spremlja zmanjšan katodni vrh v prisotnosti etanola. Anodni vrhovi imajo linearno odvisnost od kvadratnega korena stopnje skeniranja, ki je značilna za difuzijsko nadzorovane procese. Na osnovi kronoamperometričnih meritev je reakcija pokazala Cottrellianovo vedenje, difuzijski koeficient etanola pa je bil 1,26 $\times$ 10^{-5} cm^2 s^{-1}. S pomočjo impedančne spektroskopije smo prikazali elektrokatalitsko aktivnost elektrode Ni-Cu v primeru oksidacije etanola in pokazali, da se upornost napram prenosu naboja zmanjša s povečanjem koncentracije etanola.